

Estimation of the Area and Precipitation Associated with a Tropical Cyclone ‘Biparjoy’ by using Image Processing

Shikha Verma^{a,b,*}, Kuldeep Srivastava^a, Akhilesh Tiwari^b and Shekhar Verma^b

^aIndia Meteorological Department, Ministry of Earth Sciences, New Delhi, India

^bIndian Institute of Information Technology, Allahabad, Prayagraj, Uttar Pradesh, India

ARTICLE INFO

Keywords:

Tropical Cyclone
Global Precipitation Measurement
Integrated Multi-satellite Retrievals
for GPM (IMERG)
Image Processing

ABSTRACT

The rainfall associated with Tropical Cyclone (TC) contributes a major amount to the annual rainfall in India. Due to the limited research on the quantitative precipitation associated with Tropical Cyclones (TC), the prediction of the amount of precipitation and area that it may cover remains a challenge. This paper proposes an approach to estimate the accumulated precipitation and impact on affected area using Remote Sensing data. For this study, an instance of Extremely Severe Cyclonic Storm, ‘Biparjoy’ that formed over the Arabian Sea and hit India in 2023 is considered in which we have used the satellite images of IMERG-Late Run of Global Precipitation Measurement (GPM). Image processing techniques were employed to identify and extract precipitation clusters linked to the cyclone. The results indicate that Biparjoy contributed a daily average rainfall of 53.14 mm/day across India and the Arabian Sea, with the Indian boundary receiving 11.59 mm/day, covering an extensive 411.76 thousand square kilometers. The localized intensity and variability observed in states like Gujarat, Rajasthan, Madhya Pradesh, and Uttar Pradesh highlight the need for tailored response measures, emphasizing the importance of further research to enhance predictive models and disaster readiness, crucial for building resilience against the diverse impacts of tropical cyclones.

1. Introduction

Tropical Cyclones (TCs) are one of the most destructive natural disasters that affect coastal regions worldwide (Ghosh and Mistri, 2023). The 5400 km coastline of India is affected by TC of varying intensities. The North Indian Ocean (NIO) is a basin located between Africa and the Indian subcontinent and is one of the regions that experience TCs. The North Indian Ocean (NIO) basin is divided into two sub-basins, the Bay of Bengal (Bay of Bengal (BoB)) and the Arabian Sea. The Bay of Bengal sub-basin is more active than the Arabian Sea, with the majority of the TCs forming in this region. The NIO basin experiences cyclones from April to December, with the peak season occurring from September to November. The cyclones in this region are classified by the India Meteorological Department (India Meteorological Department (IMD)) scale, which takes into account the maximum sustained wind speed near the center of the cyclone.

The impacts of TCs on the NIO region are significant, including damage to infrastructure, loss of life, and economic losses. The frequency and intensity of TCs in the NIO have been observed to be increasing in recent decades. This increase in TC activity has been attributed to the rising sea surface temperatures, which provide favorable conditions for the formation and intensification of TCs (Ali, 1996; Michaels et al., 2006). The NIO region is also vulnerable to storm surges, which are caused by the combination of high

winds and low atmospheric pressure during a TC. The impact of storm surges is often more severe than the impact of the strong winds associated with TCs (Jakobsen and Madsen, 2004; Hubbert et al., 1991; Needham et al., 2015). Though the disaster caused by a TC cannot be avoided, its impact can be greatly mitigated through a variety of management approaches, such as response, recovery, prevention/reduction, and preparedness (Hoque et al., 2017). However, this makes it essential to understand the patterns and behavior of TCs in the NIO basin to improve early warning systems.

Rainfall associated with TCs has a significant impact on the environment and human activities in many regions of the world. These intense weather systems often cause severe flooding, landslides, and other hazards that can cause widespread damage to infrastructure, agriculture, and human settlements. Therefore, the study of rainfall patterns associated with TC is crucial for understanding the characteristics and behavior of these storms and their potential impact on the affected areas. This may also allow meteorologists to prepare precipitation climatology by determining the average downpour over the globe. The long-term precipitation averages may be compared against short-term precipitation events to calculate deviation. These deviations or departures from climatology are an important aspect of interpreting the changing weather patterns. This will help to assess the severity of weather phenomena that are accompanied by severe precipitation occurrences such as TC.

It was observed that in 50 years (1970-2019), floods and tropical cyclones have been two major disasters causing mortality (Ray et al., 2021). One of the most significant impacts of tropical cyclones is the abundant rainfall produced by them (Marchok et al., 2007; Rogers et al., 2009). While forecasts of TC track and intensity have improved significantly, less attention has been paid to improve the

*Corresponding author

✉ shikha.crest@gmail.com (S. Verma);

kuldeep.srivastava@imd.gov.in (K. Srivastava); atiwari@iiita.ac.in (A. Tiwari); sverma@iiita.ac.in (S. Verma)

ORCID(s): 0009-0003-5583-0431 (S. Verma)

arXiv:2407.05255v1 [cs.CV] 7 Jul 2024

estimate and forecast of the quantitative precipitation from TCs (Marchok et al., 2007; BISWAS et al., 2013; Kidder et al., 2005). It has been observed that the precipitation associated with TCs accounts for $\sim 5 - 6\%$ over the globe, $\sim 6 - 9\%$ of total precipitation over the Tropics, and about 5% over the NIO which includes both the Bay of Bengal (BoB) and the Arabian Sea (AS) (Bhatla et al., 2020; Jiang and Zipser, 2010; Lin et al., 2015).

Because of the dense population in peninsular India, the effects of TCs rainfall are more severe over the NIO (Singh et al., 2019). The spatial distribution of rainfall (Osuri et al., 2012) and the time of occurrence of rainfall (Mohapatra et al., 2013) are sensitive to cyclone tracks. The IMD and Joint Typhoon Warning Centre (JTWC), USA monitors the TCs over NIO to estimate the cyclone's path, intensity, landfall location, and time of landfall with the help of an optimal observational network, including satellite, radar, surface, and upper air observations (Mohapatra et al., 2012).

The prediction of rainfall associated with a TC is challenging because of TC's dynamic characteristics. Rainfall estimates based on manual observation, radar, Numerical Weather Prediction (NWP), and other remote sensors present intriguing opportunities for improvement. However, there has been minimal prior research confirming the model QPF performance in TCs. One of the key impediments to improving QPF in TCs is the lack of a description of the distribution of rain in space and time (Tang and Matyas, 2018).

Kidder et al. (2000) estimated the rain rate in TC with track forecasts using Tropical Rainfall Potential (TRaP) and calculated precipitation potential from Advanced Microwave Sounding Unit (Advanced Microwave Sounding Unit (AMSU)) data that appeared to be useful in forecasting the heavy precipitation associated with a landfalling TC. Lonfat et al. (2004) studied the precipitation distributions in TCs from National Aeronautics and Space Administration (NASA)'s TRMM to understand the precipitation structure of tropical cyclones and the dynamics governing the rainfall structure. In an attempt by Luitel et al. (2018), the performance of NWP was evaluated in forecasting rainfall associated with 15 U.S. landfalling TCs during the 2007-2012 period. It was observed that there was a substantial error in the precipitation prediction associated with a TC. Hence, prior to the prediction, it is important to have a detailed study on quantitative analysis of rainfall observed during the lifetime of a TC. Understanding the quantitative aspects of rainfall, such as its intensity, volume, and distribution, meteorologists can better predict and assess the potential risks associated with these cyclones, enabling them to issue timely warnings and take appropriate mitigation measures. Additionally, it is crucial for climate studies and research. Climate change is known to influence the behavior of cyclones, including their rainfall characteristics. By analyzing and quantifying rainfall patterns over time, scientists can study the impact of climate change on tropical cyclones and assess any potential changes in their behavior, such as increased rainfall rates or shifts in the distribution of rainfall.

By analyzing historical rainfall data and patterns, scientists can develop models that provide insights into the potential impact of rainfall associated with tropical cyclones, enabling authorities to issue timely warnings, plan evacuation strategies, and allocate necessary resources. Furthermore, it helps in assessing the hydrological risks associated with tropical cyclones, aiding in the design and implementation of appropriate infrastructure, drainage systems, and flood mitigation measures.

One of the basic requirements of rainfall study associated with any weather phenomenon is to identify the area of proneness on the basis of vulnerability and hazard. Since areas affected by cyclonic rainfall can be influenced by a number of factors, such as environmental humidity, low-level vorticity, vertical wind shear, TC latitude, and TC intensity (Lin et al., 2015), it is important for any country to identify the prone locations in order to lower down the adverse impact of the cyclone. In this context, the government organizations of India such as the Building Materials and Technology Promotion Council (BMTPC) and National Disaster Management Authority (NDMA) have listed vulnerable districts of different states of India based on cyclone-proneness. The IMD has identified districts for which cyclone warnings must be issued. Taking it to further, Mohapatra et al. (2012) have attempted to segregate the cyclone-prone districts of India into very high, high, moderate, and low categories of proneness. The categorization has been done on the basis of Probable Maximum Winds (PMW), Probable maximum storm surge (PMSS), and Probable maximum precipitation (PMP) for a day over any station in the district considering the other parameters such as enhanced rainfall in association with monsoon systems.

The manual observation of rainfall in the basin is not possible. Moreover, the weather radars installed at coasts have range limitations. Due to limited observations, it is difficult to accurately compute the actual rainfall that occurred over the basin during a cyclonic event. Fortunately, an earth-observing satellite Global Precipitation Measurement (GPM), provides frequent estimates of precipitation at a global scale including rainfall occurred in the basin during a cyclonic period. The Integrated Multi-satellitE Retrievals for GPM is designed to compensate for the limited sampling available from single Low-Earth-Orbit (LEO) -satellites by using as many LEO-satellites as possible, and then augmenting with Geosynchronous-Earth-Orbit (Geosynchronous-Earth-Orbit (GEO)) Infrared (IR) estimates. The IMERG system runs twice in near-real time providing "Late" multi-satellite product 14 hr after observation time and is appropriate for daily and longer applications.

In this context, an attempt has been made to provide quantitative precipitation estimation using image processing techniques over IMERG products and infer the complex relation between cyclones and associated precipitation. An instance of the Extremely Severe Cyclonic Storm, 'Biparjoy' is taken to explain the approach used in this study. The Biparjoy Cyclone occurred over the Arabian Sea and hit India in 2023. The daily average precipitation associated

with Biparjoy over the Arabian Sea and India has been estimated along with the statistics of states affected by it.

The document begins by explaining the identified problem in Section 2, shedding light on its importance. Moving on to Section 3.1, it delves into the specific geographic focus of the study, while Section 3.2 provides details about the data used. In Section 4, the step-by-step process employed to address the problem is detailed. The results are presented in Section 5, followed by an in-depth discussion in Section 6. Finally, the conclusion is presented in the Section 7.

2. Problem Description

Currently, there is a significant knowledge gap regarding TC-induced rainfall patterns, hindering precise predictions and effective mitigation strategies. The lack of specific TC-related rainfall data poses challenges in assessing the intensity and spatial distribution of precipitation within these cyclonic systems. To address this, a novel approach utilizing image processing techniques has been proposed to estimate TC-associated rainfall and its spatial distribution. The segmentation of rainfall areas within the TC system enables a quantitative assessment of rainfall extent and intensity. The significance of this research lies in improving our understanding of TC-induced rainfall and enhancing the accuracy of rainfall predictions, aiding meteorologists, disaster management agencies, and policymakers in making informed decisions. Furthermore, this research focuses specifically on the Indian region, where tropical cyclones frequently make landfall and have the potential to cause significant damage. By developing a model that can accurately estimate the rainfall patterns associated with TCs over India, this study contributes to the existing knowledge base and improves the overall understanding of cyclone dynamics in this region. This research can also serve as a foundation for further studies and advancements in TC rainfall estimation, ultimately leading to more accurate predictions and better preparedness for cyclone-related rainfall events. However, the reliance on satellite imagery introduces limitations such as potential cloud cover, image resolution, and real-time data availability, which can affect the accuracy and timeliness of rainfall estimates. Addressing these limitations is crucial for robust and accurate TC rainfall estimations.

3. Study Area and Dataset

3.1. Study Area

The study area chosen for this research is the Arabian Sea (AS) of the NIO basin as shown in shaded region of Figure 1. The AS is divided into 6 zones namely NWA, NEA, WCA, ECA, SWA, and SEA. The region is known to be prone to tropical cyclones, particularly during the pre-monsoon and post-monsoon seasons, and therefore, it is important to understand the behavior of these cyclones to better prepare and mitigate their impacts. The cyclogenesis of tropical cyclone Biparjoy of Extremely Severe Cyclonic Storm (Extremely Severe Cyclonic Storm (ESCS)) category was observed in AS on 06-06-2023, which was the first

Cyclonic Storm (CS) over the Arabian Sea in the year 2023. As per the report of IMD, it crossed Saurashtra and Kutch coast close to Jakhau Port near latitude 23.28°N and longitude 68.56°E with Maximum Sustained Wind (MSW) of 65 knots gusting to 75 knots on 15-06-2023. Finally, it weakened into a depression (Depression (D)) over South Rajasthan and adjoining North Gujarat on 18-06-2023 and into a WML over central parts of Northeast Rajasthan and neighbourhood on 19-06-2023 at 03 UTC.

3.2. Dataset

The GPM_3IMERGHHL (GPM IMERG Late Precipitation L3 Half Hourly) dataset has been selected as the primary data set for this study. This choice is motivated by the dataset's capability to provide comprehensive and detailed information on precipitation dynamics. Utilizing advanced algorithms such as GPROF2017, the dataset offers half-hourly precipitation estimates with a spatial resolution of $0.1^\circ \times 0.1^\circ$. Notably, the inclusion of "late" observations, occurring around 14 hours after the initial observation time, adds temporal depth to the dataset. The meticulous processing, including gridding, intercalibration to the GPM Combined Ku Radar-Radiometer Algorithm (CORRA) product, and bias correction, enhances the dataset's accuracy and reliability, making it an ideal choice for the study's comprehensive analysis of precipitation patterns (NASA GES DISC, 2019).

In adherence to the WMO standards, this study considers the Date of Acquisition (DOA) for 24-hour precipitation from 07-06-2023 to 20-06-2023 recorded at 03 UTC to ensure a consistent and uniform observation protocol. The detail of the dataset along with Date_id (D_ID) is listed in Table 1 and will be used as a nomenclature in the further sections.

4. Methodology

The proposed method uses satellite imagery to analyze rainfall and determine the extent of the Biparjoy cyclone's

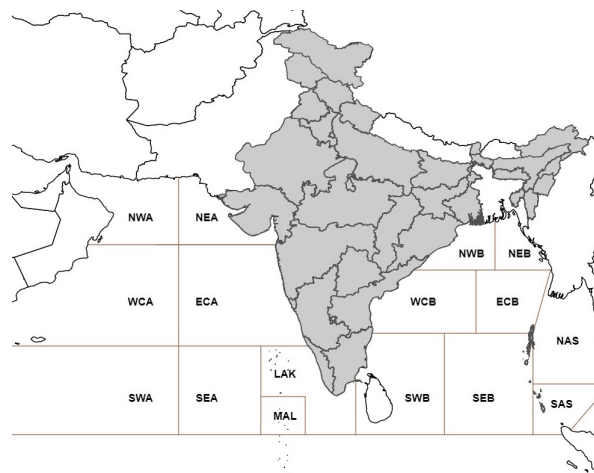


Figure 1: Study area

Table 1: Details of the dataset used

SN	Date of Acquisition (DOA)	D_ID
1	07-06-2023	D1
2	08-06-2023	D2
3	09-06-2023	D3
4	10-06-2023	D4
5	11-06-2023	D5
6	12-06-2023	D6
7	13-06-2023	D7
8	14-06-2023	D8
9	15-06-2023	D9
10	16-06-2023	D10
11	17-06-2023	D11
12	18-06-2023	D12
13	19-06-2023	D13
14	20-06-2023	D14

coverage. By processing the satellite data using image processing techniques, we can identify specific rainfall patterns and understand the impact of the cyclone more accurately. This approach overcomes the limitations of traditional methods and provides a clearer picture of the cyclone's effects, even in areas with limited ground-based observations. Hence, it offers a more comprehensive understanding of the cyclone's impact and enables improved decision-making and response strategies.

The step-wise workflow of the proposed approach is shown in Figure 2. It shows that the data is downloaded which is pre-processed for further processing. Then, the mask of the precipitation blob has been generated from which the major blob was extracted based on the connected component. The precipitation from the extracted cluster has been computed for the study site. Based on the spatial resolution of IMERG data of rainfall, the total area affected by rainfall associated with cyclone 'Biparjoy' in India has been computed. A comprehensive explanation of each step is given below.

4.1. Data download

The IMERG product GPM_3IMERHHL v06 is downloaded from the data server of NASA. The details of the dataset are given in section 3.2. IMERG (Integrated Multi-satellite Retrievals for GPM) is a unified satellite precipitation product that provides estimated surface precipitation over most of the globe. It is a product of Global Precipitation Measurement (GPM), which is an international satellite mission jointly launched by NASA and Japan Aerospace Exploration Agency (JAXA) to provide unified precipitation measurements of rain and snow every three hours.

4.2. Pre-processing

In this section, the pre-processing steps for the downloaded data are explained. The pre-processing steps ensure that the data is in the appropriate format and ready for further analysis. These steps are important in any analysis involving

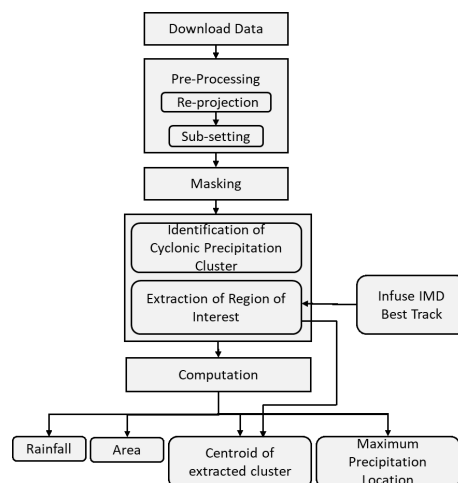


Figure 2: Workflow of the proposed approach

geospatial data, as they can significantly impact the accuracy and reliability of the results.

The first step in pre-processing is re-projection, which involves warping the images from their original projection space to a selected projection space. This process requires the calculation of a geometric transformation model, which accounts for the relative geometry of the two projections and local scale and resolution changes in the images. The amount of distortion incurred during re-projection depends on these factors. In this study, the projection of downloaded raster data is converted from sinusoidal to geographic latitude-longitude for further processing (Steinwand et al., 1995).

The next step in pre-processing is spatial subsetting, which involves extracting the region of interest (ROI). This process returns a new object with only features that are spatially related to the Region of Interest (ROI) (Ayoobi and Tangestani, 2017). This step is important because it reduces the data size and processing time, making it easier to analyze the data. Figure 3 shows the images for D1 to D14 after re-projection and spatial subsetting.

4.3. Masking

After the pre-processing step, a two-step thresholding approach is employed to filter out irrelevant information and highlight the crucial features in the satellite imagery. Initially, pixels with values exceeding 0.9 mm are masked out, focusing on regions where precipitation is significant. Subsequently, a finer threshold of 0.3 mm is employed, emphasizing the areas with a more pronounced cyclonic structure. This sequential approach ensures that the masking strategy evolves from a broader emphasis on significant precipitation to a more nuanced focus, particularly when the cyclone's eye becomes prominent. The outcome of this process is a binary mask image, which contains pixels with either a value of 0 or 1, representing the areas that meet the specified condition and those that do not. To visually represent the effectiveness of this preprocessing step, the masked images for the D1 to D14 are shown in Figure 4.

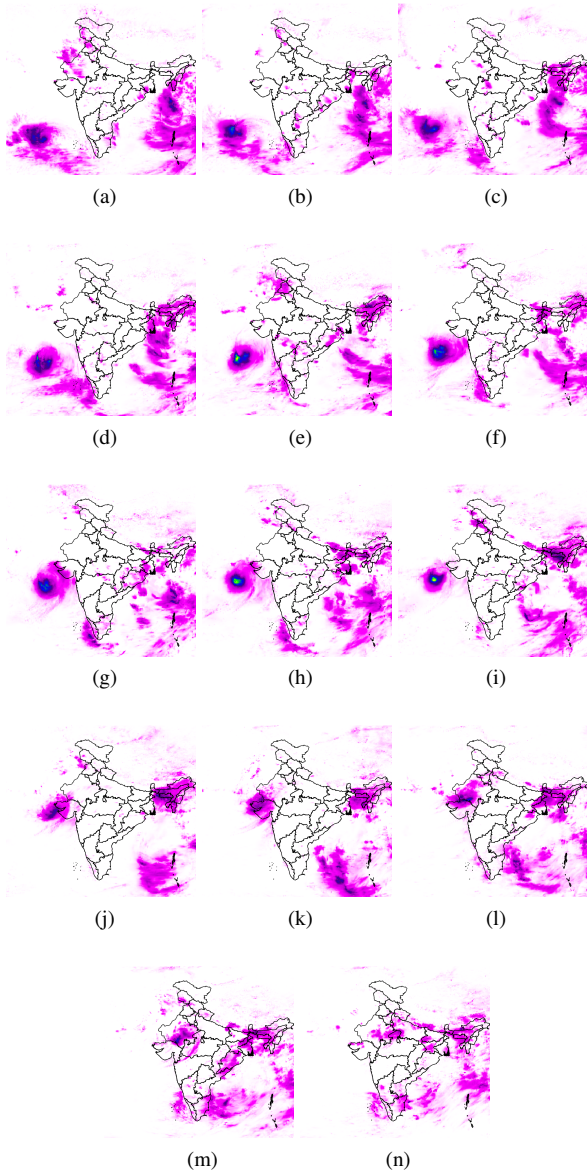


Figure 3: Pre-processed images for the D_ID (a)-(n): D1-D14

4.4. Identification and Extraction of Cyclonic Precipitation Cluster

In this step of the study, the focus is on labeling the results obtained from the previous step based on the area they cover. The objective is to identify the precipitation clusters associated with the Biparjoy cyclone, which can then be further processed. The employed methodology involves leveraging Connected Component Analysis (Connected Component Analysis (CCA)). This technique is utilized to effectively identify and label connected regions within a binary image, enabling a detailed examination of the precipitation patterns associated with the cyclone. It involves finding the objects in a binary image by creating a labeled image where pixels with identical integer values belong to the same class of object. The algorithm works by scanning the binary image

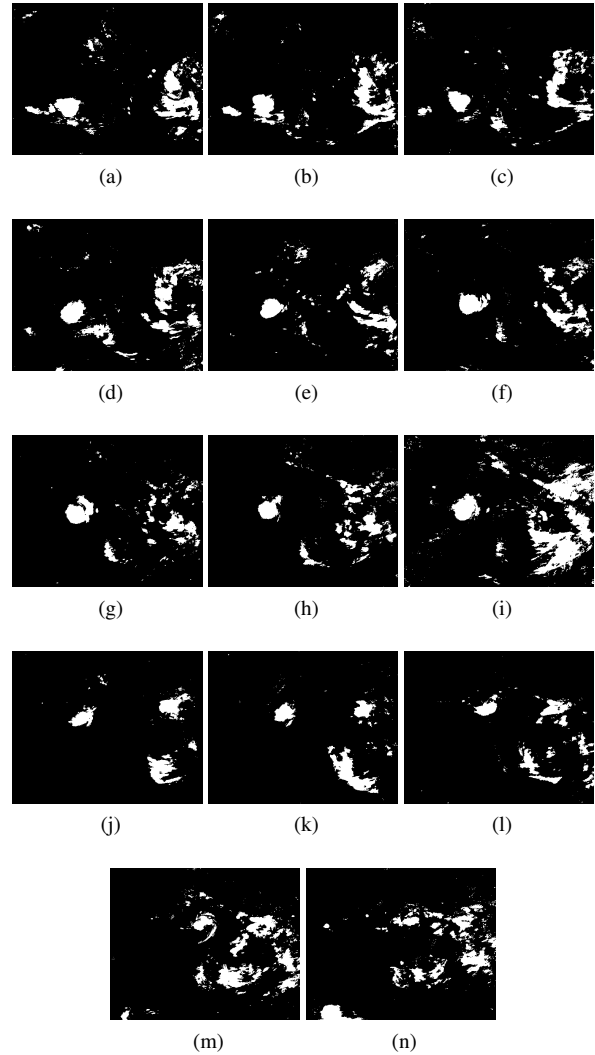


Figure 4: Cloud mask for D_ID (a)-(n): D1-D14

pixel by pixel and checking whether each pixel is connected to any of its neighbors. A pixel is considered connected to its neighbors if they have the same value, and they are adjacent to each other either horizontally or vertically. When a group of connected pixels is identified, they are assigned a unique label, and the process is repeated until all pixels in the image have been labeled. The result of the CCA algorithm is a labeled image, where each cluster of connected pixels is assigned a unique label. This labeled image can then be used for further analysis and processing. Mathematically, the CCA algorithm can be represented by the following equation:

$$L = bwlabel(BW)$$

where L is the labeled image, BW is the binary image, and $bwlabel$ is the function that performs the CCA operation. The function $bwlabel$ assigns a unique integer label to each connected cluster of pixels in the binary image BW .

In the present study, the binary image represents the precipitation clusters associated with the cyclone. The False

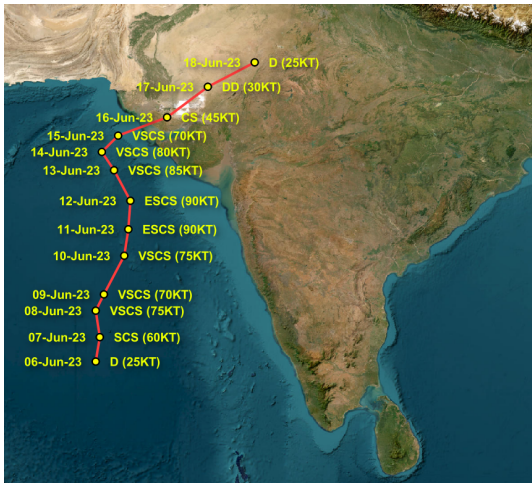


Figure 5: Best Track of Biparjoy Cyclone

value in the binary image represents background pixels, while the True value represents object pixels.

Moreover, to ascertain the precise association of identified precipitation clusters with the Biparjoy cyclone and to mitigate any potential ambiguity arising from other weather events in the region, we are incorporating the best track information of 03 UTC provided by the IMD, as illustrated in Figure 5. This meticulous consideration of the Biparjoy cyclone’s best track is essential for the accurate labeling of the identified precipitation clusters, laying a crucial foundation for the subsequent in-depth analysis of the associated rainfall patterns.

The extracted images of cyclonic precipitation clusters so obtained are shown in Figure 6. These images serve as pivotal visual aids for further analysis and interpretation of the cyclonic activity attributed to the Biparjoy. Moving forward, Figure 7, presents a vector image of the study area projected onto the extracted cyclonic precipitation clusters, which effectively illustrates the distribution of precipitation in various Indian states.

Having identified and labeled the cyclonic precipitation clusters, the subsequent step involves computing pertinent statistics associated with these clusters. Specifically, the total precipitation associated with the Biparjoy cyclone is computed by summing up the precipitation values within the identified clusters. Additionally, the total area affected by the clusters and the total area of the affected states is also computed for each day. These computed metrics provide valuable insights into the cyclone’s impact on the affected regions, offering essential information for disaster response and management efforts.

5. Result

In this section, we estimate the total rainfall associated with cyclone Biparjoy on each day along with the area covered by it. Moreover, the centroid of extracted precipitation cluster and Maximum Rainfall Point are computed. Thereafter, the result is analyzed and discussed in detail.

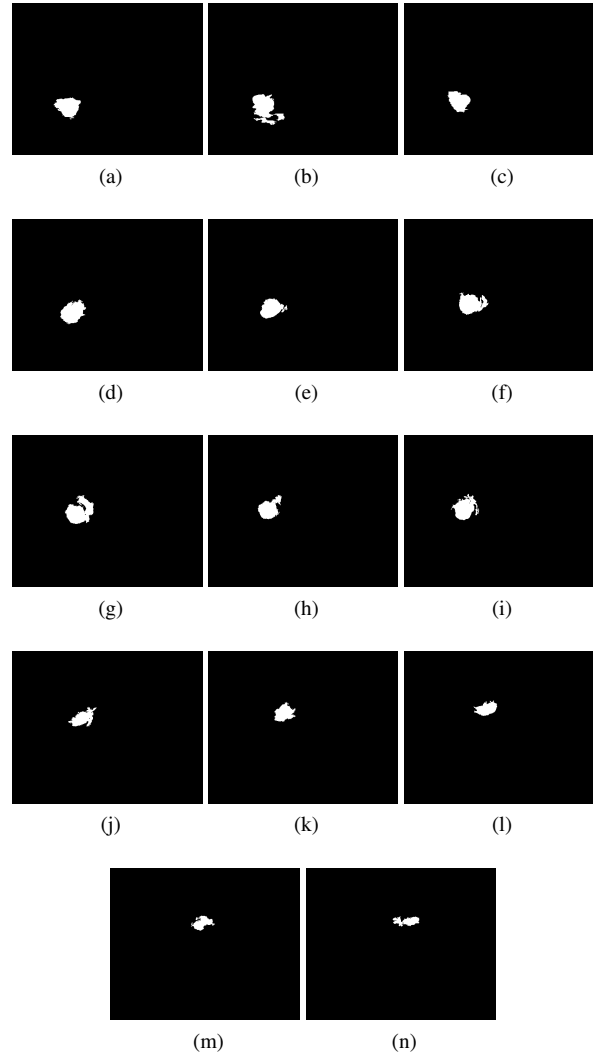


Figure 6: Extracted Cyclonic Precipitation Clusters for the D_ID (a)-(n): D1-D14

5.1. Pixel Count

The pixel counts in the processing of IMERG product containing the number of pixels in the mask and the number of pixels in extracted precipitation clusters after applying image processing techniques from D1 to D14 are shown in Figure 8.

The analysis of the pixel data in conjunction with the distinctive characteristics of Cyclone Biparjoy reveals intricate relationships between meteorological phenomena and the observed variations in precipitation clusters. On analyzing 8, the findings reveal significant insights into the spatial distribution of precipitation clusters associated with the Biparjoy cyclone. Notably, the count of pixels within the binary mask consistently exceeds the count of pixels in the extracted precipitation cluster. This discrepancy is indicative of areas within the mask that do not contribute to the identified precipitation clusters. Further investigation indicates that a subset of pixels in the mask is associated with convection patterns related to the cross Equatorial southwest

Precipitation Associated with Biparjoy

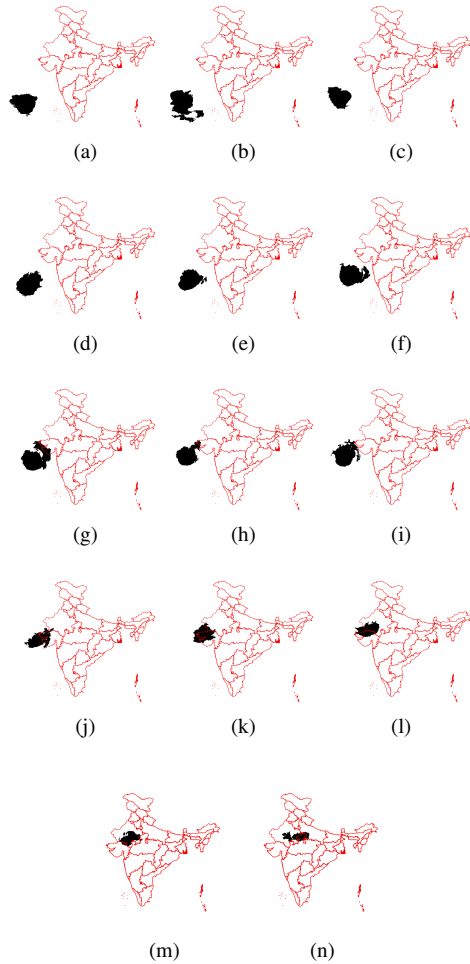


Figure 7: Visualization of Extracted Cyclonic precipitation cluster over the boundary of India for the D_ID (a)-(n): D1-D14

monsoon flow over the southeast Arabian Sea. Additionally, the rainfall observed over the Kerala and Lakshadweep area is attributed to the onset of the southwest monsoon, which commenced over most parts of Kerala and the entire Lakshadweep on June 8th.

The temporal evolution of the pixel counts provides valuable information about the dynamic nature of precipitation clusters throughout the observed period. On D9, we observe a notable increase in the number of pixels within the binary mask, suggesting an intensification of weather patterns. This escalation is likely attributed to a weather phenomenon occurring over North-Eastern part of India. Concurrently, the count of pixels in the extracted precipitation cluster remains relatively consistent, signifying a concentration of precipitation in specific regions. Furthermore, the diurnal fluctuations in convective clouds, further emphasize the dynamic nature of the precipitation clusters, reflected in the pixel counts.

Following landfall, the sustained pixel counts within the binary mask and extracted precipitation cluster illustrate the cyclone's persistence even after making landfall. These

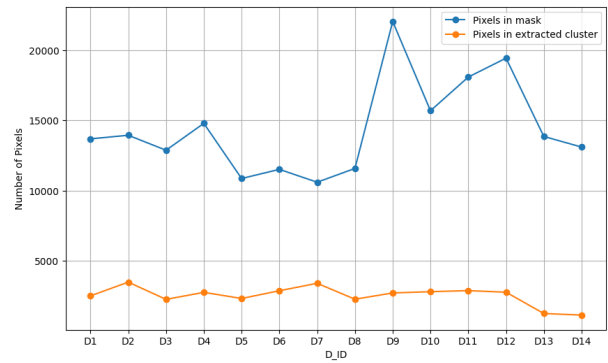


Figure 8: Pixel Count of Mask and Extracted Cyclonic Precipitation Cluster

pixel trends reflect the post-landfall intensity and gradual weakening till midnight of June 16th, providing a visual representation of the cyclone's behavior.

Consistently, the pixel data reveals variations, underscoring the complexity of Cyclone Biparjoy and the challenges in predicting its path. The interconnectedness of pixel variations and meteorological characteristics highlights the potential for advanced methodologies in pixel segmentation and the integration of additional data sources for a more comprehensive understanding of cyclonic events. This holistic approach contributes to improved forecasting and enhanced disaster management capabilities.

5.2. Estimation of Rainfall

Since the IMERG product acquires data from sparse locations, the rainfall data of cyclones over the ocean is available. After pre-processing, the total rain due to the Biparjoy cyclone has been computed. Knowing the total rainfall over India after landfall is important to prepare the rainfall climatology. Therefore, the day-wise total rainfall and the corresponding area are computed before and after landfall over India by using Simple Mean Method. Though the Simple Mean method is easy to use and provides a quick estimate of the average value, it has limitations in situations where the data is highly skewed or contains outliers.

On the basis of extracted cyclonic precipitation cluster, the average daily rainfall is calculated over India by using Simple Mean. In this calculation, rainfall measurements greater than 0.1mm are considered significant, while measurements less than or equal to 0.1mm are considered as trace. The result is shown in Figure 9.

Figure 9 provides an insight into the variation of average daily rainfall during the Biparjoy cyclone event and highlights the importance of considering both the extracted cyclonic precipitation cluster and the area over which the rainfall is averaged when analyzing rainfall patterns.

The daily average rainfall due to Cyclone Biparjoy, computed from the extracted precipitation clusters, stands at 53.14 mm/day, encompassing both India and the Arabian Sea region, whereas the Indian boundary received an average of 11.59 mm/day. This aggregated metric serves as a key

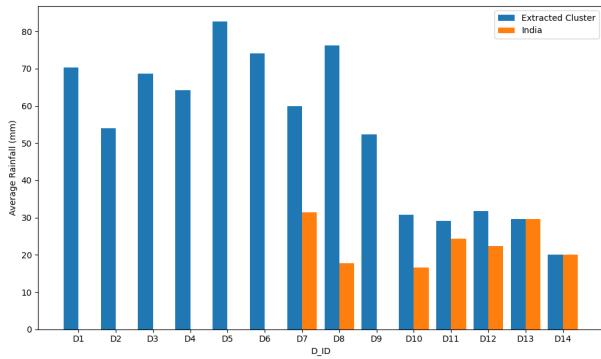


Figure 9: Average Daily Rainfall due to Biparjoy Cyclone over India

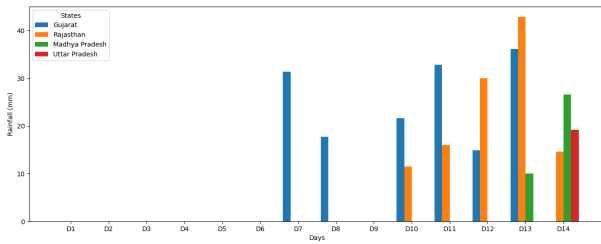


Figure 10: Rainfall received by different states of India

indicator of the overall intensity and extent of precipitation influenced by Cyclone Biparjoy during the analyzed time-frame. Upon closer examination of the broader geographical scope, the impact on India as a whole is characterized by significant variations in rainfall patterns across different states.

During the influence of Cyclone Biparjoy, four states were significantly affected namely Gujarat, Rajasthan, Madhya Pradesh, and Uttar Pradesh experiencing distinct patterns of precipitation as depicted in Figure 10. Cyclone Biparjoy made landfall on D6 along the coast of Gujarat, marking a significant meteorological event. The impact of the cyclone on Gujarat was the most pronounced impact across 6 days, marked by a substantial 31.25 mm/day downpour on D7 and an average daily rainfall of 11.03 mm/day. This rainfall persisted in Gujarat on the subsequent day, showcasing the sustained influence of Cyclone Biparjoy on the region. Intriguingly, on D9, a temporary respite from rainfall was observed over the entire Indian region. However, this reprieve was short-lived as the cyclone resumed affecting Gujarat and extended its impact to Rajasthan from the following day onwards. The meteorological data indicates a noteworthy shift in the cyclone’s trajectory and influence. The absence of recorded rainfall over India on D9 signifies a brief interlude in the cyclone’s activity, offering a temporary relief from precipitation across the country. Nevertheless, the subsequent resurgence of rainfall, specifically impacting Gujarat and Rajasthan, underscores the dynamic nature of Cyclone Biparjoy’s trajectory and its ability to affect diverse regions over time. Rajasthan, spanning 5 days, experienced peak precipitation on D13, recording a notable

42.89 mm/day rainfall, with an average daily rainfall of 8.21 mm. Madhya Pradesh, impacted over 2 days, observed its highest precipitation of 10.05 mm on D13, featuring an average daily rainfall of 2.62 mm/day. Similarly, Uttar Pradesh, affected for 1 day, witnessed peak rainfall of 19.15 mm/day on D14, displaying a comparatively lower average daily rainfall of 1.37 mm/day. Notably, Rajasthan received the highest single-day rainfall among the four states, recording 42.89 mm/day on D13. This information emphasizes the localized intensity and variability of precipitation during the cyclone’s impact on different regions. The state-specific statistics provide a comprehensive and detailed assessment of Biparjoy’s influence on regional precipitation patterns. These detailed insights play a pivotal role in formulating well-informed disaster management and response strategies tailored to the specific impact experienced by each state, enhancing overall preparedness and resilience.

5.3. Estimation of Area Covered

In this step, we conducted a thorough analysis of the spatial distribution of rainfall during the Biparjoy cyclone, aiming to understand its impact on different regions. To achieve this, we calculated the total area covered by the precipitation cluster over India. The results are visually presented in Figure 11, providing valuable insights into the geographical extent of rainfall associated with the cyclone.

The comprehensive area covered by the Biparjoy cyclone was determined by unifying all the extracted raster images. The union operation allowed us to merge these individual clusters, providing a consolidated view of the spatial extent of precipitation associated with the cyclone. This approach ensures that the cumulative impact area is accurately captured, considering the evolving nature of the cyclone over time. This methodology contributes to a comprehensive analysis of the cyclone’s influence on various regions, laying the groundwork for a thorough understanding of its spatial and temporal characteristics.

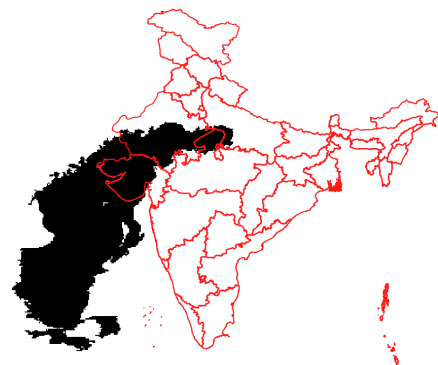


Figure 11: Area Covered by Biparjoy Cyclone over Arabian Sea and India

In the course of our analysis of Cyclone Biparjoy’s impact on different regions, we meticulously examined the daily coverage area across Gujarat, Rajasthan, Madhya

Precipitation Associated with Biparjoy

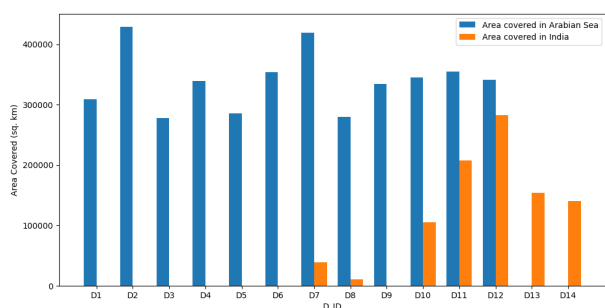


Figure 12: Total Area Covered by Extracted Precipitation Cluster of Biparjoy Cyclone and Over India

Pradesh, and Uttar Pradesh. The visual representation is shown in 12.

Our findings reveal that the Biparjoy covered a substantial 411.76 thousand square kilometers in total, with Gujarat experiencing an impact over 154.75 thousand square kilometers, followed by Rajasthan with 194.80 thousand square kilometers. Madhya Pradesh and Uttar Pradesh were also significantly affected, with impact areas of 40.78 and 21.43 thousand square kilometers, respectively.

Throughout the progression of Cyclone Biparjoy, distinct patterns of precipitation coverage were observed. On D7 and D8, a notable area of Gujarat, totaling 39.1 thousand sq. km, experienced the impact of the cyclone. Subsequently, the influence intensified on D10 and D11, extending to cover substantial regions in Gujarat, Rajasthan, and Madhya Pradesh. The zenith of the cyclone's impact was observed on D11, with widespread precipitation exceeding 150.7 thousand sq. km in Gujarat and 57.3 thousand sq. km in Rajasthan. This impactful trend persisted on D12 and D13, revealing significant coverage in Gujarat, Rajasthan, and Madhya Pradesh.

Madhya Pradesh, in particular, witnessed substantial coverage from D12 to D14, recording precipitation areas of 207.0 thousand sq. km, 138.9 thousand sq. km, and 77.9 thousand sq. km, respectively. Even on the concluding day (D14), as the cyclone's influence gradually diminished, a considerable area remained covered in Rajasthan, Madhya Pradesh, and Uttar Pradesh, highlighting the lasting effect of Cyclone Biparjoy across these regions. Notably, Rajasthan sustained coverage of 40.8 thousand sq. km, while Uttar Pradesh experienced precipitation over an area of 21.4 thousand sq. km. This detailed analysis provides valuable insights into the temporal progression of the cyclone and its varying impact on different states, contributing to our understanding for further research and disaster management strategies.

6. Discussion

In this study, we estimated the quantitative precipitation associated with cyclone Biparjoy which provided insights into the spatial distribution of the rainfall and its impact on the affected areas. We used image processing techniques

on IMERG raster data to identify and extract precipitation clusters associated with the Biparjoy cyclone. Specifically, we computed the total rainfall for each day and also determined the area covered by the cyclone. We then proceeded to conduct a detailed analysis of the results obtained.

The findings of this study provide a significant contribution to the understanding of Cyclone Biparjoy's impact on precipitation patterns across India. The daily average rainfall of 53.14 mm/day reflects the cyclone's substantial influence, with Gujarat experiencing a particularly pronounced impact, marked by a peak daily rainfall of 31.25 mm on D7. The dynamic trajectory of the cyclone resulted in varying levels of impact on different states, showcasing the complexity of cyclonic behavior. The spatial distribution analysis further underscores the extensive coverage area of 411.76 thousand square kilometers, emphasizing the far-reaching impact of Cyclone Biparjoy.

The temporal progression of the cyclone's influence, as revealed through this study, sheds light on the resilience and adaptability of disaster management strategies. The localized intensity and variability observed in states like Gujarat, Rajasthan, Madhya Pradesh, and Uttar Pradesh highlight the need for tailored response measures to address the diverse impacts of cyclones on different regions. The short-lived reprieve from rainfall on D9 and the subsequent resurgence underscore the challenges in predicting and managing cyclonic behavior.

This study's insights provide a foundation for future research and contribute to the development of more targeted disaster preparedness and response strategies. The nuanced understanding of cyclonic dynamics, as presented in this research, is crucial for enhancing the overall resilience of communities and infrastructure in the face of such meteorological events.

7. Conclusion

Our study highlighted the significant impact of tropical cyclone Biparjoy on precipitation over India and the need for further research to better understand the dynamics and implications for regional precipitation. This study urges further investigations to improve predictive models, enhance disaster readiness, and develop specific responses. Such efforts are vital for building resilience against the diverse impacts of tropical cyclones in the changing climate scenario.

Acknowledgement

The author would like to express my heartfelt gratitude to the India Meteorological Development (IMD) and the Indian Institute of Information Technology, Allahabad (IIIT Allahabad) for their invaluable support and contributions to this journal. Their guidance, resources, and assistance have been instrumental in the successful completion of this research.

Abbreviations

AMSU Advanced Microwave Sounding Unit

BMTPC Building Materials and Technology Promotion Council

BoB Bay of Bengal

CCA Connected Component Analysis

CS Cyclonic Storm

D Depression

DOA Date of Acquisition

ESCS Extremely Severe Cyclonic Storm

GEO Geosynchronous-Earth-Orbit

GPM Global Precipitation Measurement

IMD India Meteorological Department

IMERG Integrated Multi-satellitE Retrievals for GPM

IR Infrared

JAXA Japan Aerospace Exploration Agency

JTWC Joint Typhoon Warning Centre

LEO Low-Earth-Orbit

MSW Maximum Sustained Wind

NASA National Aeronautics and Space Administration

NDMA National Disaster Management Authority

NIO North Indian Ocean

NWP Numerical Weather Prediction

ROI Region of Interest

TC Tropical Cyclones

TCs Tropical Cyclones

References

- S. Ghosh, B. Mistri, Cyclone-induced coastal vulnerability, livelihood challenges and mitigation measures of matla–bidya inter-estuarine area, indian sundarban, *Natural Hazards* 116 (2023) 3857–3878.
- A. Ali, Vulnerability of Bangladesh to climate change and sea level rise through tropical cyclones and storm surges, Springer, 1996.
- P. J. Michaels, P. C. Knappenberger, R. E. Davis, Sea-surface temperatures and tropical cyclones in the atlantic basin, *Geophysical Research Letters* 33 (2006).
- F. Jakobsen, H. Madsen, Comparison and further development of parametric tropical cyclone models for storm surge modelling, *Journal of Wind Engineering and Industrial Aerodynamics* 92 (2004) 375–391.
- G. D. Hubbert, G. J. Holland, L. M. Leslie, M. J. Manton, A real-time system for forecasting tropical cyclone storm surges, *Weather and Forecasting* 6 (1991) 86–97.
- H. F. Needham, B. D. Keim, D. Sathiaraj, A review of tropical cyclone-generated storm surges: Global data sources, observations, and impacts, *Reviews of Geophysics* 53 (2015) 545–591.
- M. A.-A. Hoque, S. Phinn, C. Roelfsema, I. Childs, Tropical cyclone disaster management using remote sensing and spatial analysis: A review, *International journal of disaster risk reduction* 22 (2017) 345–354.
- K. Ray, R. Giri, S. Ray, A. Dimri, M. Rajeevan, An assessment of long-term changes in mortalities due to extreme weather events in india: A study of 50 years' data, 1970–2019, *Weather and Climate Extremes* 32 (2021) 100315.
- T. Marchok, R. Rogers, R. Tuleya, Validation schemes for tropical cyclone quantitative precipitation forecasts: Evaluation of operational models for us landfalling cases, *Weather and forecasting* 22 (2007) 726–746.
- R. Rogers, F. Marks, T. Marchok, Tropical cyclone rainfall, *Encyclopedia of hydrological sciences* 3 (2009).
- H. BISWAS, P. Kundu, D. Pradhan, A case study for cyclone 'aila' for forecasting rainfall using satellite derived rain rate data, *Mausam* 64 (2013) 77–82.
- S. Q. Kidder, J. A. Knaff, S. J. Kusselson, M. Turk, R. R. Ferraro, R. J. Kuligowski, The tropical rainfall potential (trap) technique. part i: Description and examples, *Weather and Forecasting* 20 (2005) 456–464.
- R. Bhatla, R. Raj, R. Mall, Shivani, Tropical cyclones over the north indian ocean in changing climate, *Techniques for disaster risk management and mitigation* (2020) 63–76.
- H. Jiang, E. J. Zipser, Contribution of tropical cyclones to the global precipitation from eight seasons of trmm data: Regional, seasonal, and interannual variations, *Journal of climate* 23 (2010) 1526–1543.
- Y. Lin, M. Zhao, M. Zhang, Tropical cyclone rainfall area controlled by relative sea surface temperature. *nat. commun.*, 6, 6591, 2015.
- K. Singh, M. Mandal, P. K. Bhaskaran, Impact of radiance data assimilation on the prediction performance of cyclonic storm sidr using wrf-3dvar modelling system, *Meteorology and Atmospheric Physics* 131 (2019) 11–28.
- K. K. Osuri, U. Mohanty, A. Routray, M. A. Kulkarni, M. Mohapatra, Customization of wrf-arw model with physical parameterization schemes for the simulation of tropical cyclones over north indian ocean, *Natural Hazards* 63 (2012) 1337–1359.
- M. Mohapatra, D. Nayak, R. Sharma, B. Bandyopadhyay, Evaluation of official tropical cyclone track forecast over north indian ocean issued by india meteorological department, *Journal of Earth System Science* 122 (2013) 589–601.
- M. Mohapatra, B. Bandyopadhyay, A. Tyagi, Best track parameters of tropical cyclones over the north indian ocean: A review, *Natural Hazards* 63 (2012) 1285–1317.
- J. Tang, C. Matyas, A nowcasting model for tropical cyclone precipitation regions based on the trec motion vector retrieval with a semi-lagrangian scheme for doppler weather radar, *Atmosphere* 9 (2018) 200.
- S. Q. Kidder, M. D. Goldberg, R. M. Zehr, M. DeMaria, J. F. Purdom, C. S. Velden, N. C. Grody, S. J. Kusselson, Satellite analysis of tropical cyclones using the advanced microwave sounding unit (amsu), *Bulletin of the American Meteorological Society* 81 (2000) 1241–1260.
- M. Lonfat, F. D. Marks Jr, S. S. Chen, Precipitation distribution in tropical cyclones using the tropical rainfall measuring mission (trmm) microwave imager: A global perspective, *Monthly Weather Review* 132 (2004) 1645–1660.
- B. Luitel, G. Villarini, G. A. Vecchi, Verification of the skill of numerical weather prediction models in forecasting rainfall from us landfalling tropical cyclones, *Journal of hydrology* 556 (2018) 1026–1037.
- M. Mohapatra, G. Mandal, B. Bandyopadhyay, A. Tyagi, U. Mohanty, Classification of cyclone hazard prone districts of india, *Natural hazards* 63 (2012) 1601–1620.
- NASA GES DISC, GPM IMERG late precipitation L3 1 day 0.1 degree x 0.1 degree V06, 2019. URL: https://disc.gsfc.nasa.gov/datasets/GPM_3IMERGHHLL_06/summary.
- D. Steinwand, J. Hutchinson, J. Snyder, Map projections for global and continental data sets and an analysis of pixel distortion caused by reprojection. *photogramm. eng. Rem. S* 61 (1995) 1–487.

- I. Ayoobi, M. H. Tangestani, Evaluating the effect of spatial subsetting on subpixel unmixing methodology applied to aster over a hydrothermally altered terrain, *International journal of applied earth observation and geoinformation* 62 (2017) 1–7.